Optics Letters

Low-cost single-point optoacoustic sensor for spectroscopic measurement of local vascular oxygenation

Antonios Stylogiannis,[1,2] **Lucas Riobo,**[1,2] **Ludwig Prade,**[1,2] **Sarah Glasl,**[1,2]
Sabine Klein,[3] **Giulia Lucidi,**[4] **Martin Fuchs,**[4] **Dieter Saur,**[3] and
Vasilis Ntziachristos[1,2,*]

[1]*Technical University of Munich, Chair of Biological Imaging, Munich, Germany*
[2]*Helmholtz Zentrum München, Institute of Biological and Medical Imaging, Oberschleißheim, Germany*
[3]*Technical University of Munich, Germany, Translational Cancer Research and experimental Cancer Therapy, Munich, Germany*
[4]*iTheraMedical GmbH, Zielstattstrasse 13, 81379 Munich, Germany*
Corresponding author: bioimaging.translatum@tum.de

Optical sensors developed for the assessment of oxygen in tissue microvasculature, such as those based on near-infrared spectroscopy, are limited in application by light scattering. Optoacoustic methods are insensitive to light scattering, and therefore, they can provide higher specificity and accuracy when quantifying local vascular oxygenation. However, currently, to the best of our knowledge, there is no low-cost, single point, optoacoustic sensor for the dedicated measurement of oxygen saturation in tissue microvasculature. This work introduces a spectroscopic optoacoustic sensor (SPOAS) for the non-invasive measurement of local vascular oxygenation in real time. SPOAS employs continuous wave laser diodes and measures at a single point, which makes it low-cost and portable. The SPOAS performance was benchmarked using blood phantoms, and it showed excellent linear correlation ($R^2 = 0.98$) with a blood gas analyzer. Subsequent measurements of local vascular oxygenation in living mice during an oxygen stress test correlated well with simultaneous readings from a reference instrument. © 2020 Optical Society of America under the terms of the OSA Open Access Publishing Agreement

https://doi.org/10.1364/OL.412034

Arterial blood oxygenation is routinely assessed in clinics by either invasive electrochemical means, i.e., using a blood gas analyzer (BGA), or by non-invasive optical means, i.e., using a pulse oximeter. In contrast to arterial blood oxygenation, tissue oxygenation is the partial pressure of oxygen within the interstitial spaces of a particular tissue [1]. Each organ has its own oxygenation status, depending in its size and function [2], and abnormalities in tissue oxygenation may indicate hypoxia associated with occlusions, vascular damage, cardiovascular disease, diabetes, or cancer [3]. Moreover, information on tissue oxygenation is valuable in critical situations, such as during surgery (anastomosis, tissue perfusion, transplantation, etc.),

in the emergency room and rescue operations, and for patient monitoring in the intensive care unit [4]. Tissue oxygenation is generally measured by polarographic and dynamic fluorescence quenching methods, but these techniques require invasive probes and are thus impractical for *in vivo* clinical work. Furthermore, tissue oxygenation cannot be directly inferred from arterial blood oxygenation measurements, as there is poor correlation between both instantaneous and average arterial blood and the tissue oxygenation values [1].

In contrast to tissue oxygenation, local vascular oxygenation—the average hemoglobin saturation in the arterioles and venules within a defined region—can be probed non-invasively using optical methods that exploit the different absorption profiles of oxyhemoglobin and deoxyhemoglobin. Furthermore, unlike arterial oxygenation, local vascular oxygenation is organ specific and results from the balance between the local oxygen delivery from the blood to the tissue and the oxygen consumption by the cells. Thus, it correlates more closely with tissue oxygenation [1,2]. Techniques based on near-infrared spectroscopy (NIRS) have been developed to image or sense the local vascular oxygenation at different points in the tissue or different organs, such as in the brain, muscles, or the splanchnic region [5,6]. However, NIRS-based techniques are inherently limited by their reliance on the detection of NIR light, which is strongly scattered and absorbed by multiple chromophores in tissue, such as melanin, fat, hemoglobin, etc. The strong scattering leads to large minimum sample volumes ($\sim 1.5\ cm^3$), which contain mixed contributions of multiple tissue components [7]. Because of these major limitations, detected signals are also inherently weak, making quantification of local vascular oxygenation with NIRS challenging. These quantification issues have limited the wide dissemination of the NIRS-base techniques to clinical environments. The widely used pulse oximeter overcomes some of these limitations by measuring only the pulse-induced variation in the absorption

of NIR light by arterial blood in the fingertip. However, the pulse oximeter requires a strong, steady pulse, which limits its use when patients present with conditions that limit blood flow, such as vasoconstriction (e.g., in cold environments), low blood pressure, cardiac arrhythmia, and venous congestion [8].

Similar to NIRS, optoacoustic (OA, also photoacoustic) methods [9] can also exploit the characteristic absorption profiles of oxyhemoglobin and deoxyhemoglobin to measure local vascular oxygenation [10]. However, OA methods overcome the NIRS major limitation by detecting acoustic waves (rather than transmitted light), which are not significantly absorbed or scattered in the tissue. Acoustic detection enables OA methods to resolve depth with a higher axial resolution than NIRS, and thus measure oxygenation in smaller and deeper volumes with more specificity [10]. The insensitivity to scatter also enables higher accuracy quantification of local vascular oxygenation than purely optical methods that use diffusive light [11]. However, multispectral OA systems [12] typically employ a high energy, multispectral laser source, making them expensive and bulky, and therefore ill-suited for point-of-care or bedside applications.

Low-cost OA imaging and sensing systems have been developed, which employ laser diodes (LD) or light-emitting diodes (LED) as illumination sources [13]. However, a variety of design elements make these systems impractical for low-cost single-point sensing of local vascular oxygenation. For instance, one commercially available system incorporates 4 rows of 36 LED arrays (144 total elements) at different wavelengths between 470 nm and 850 nm, as well as a 128 element ultrasound (US) array for combined US and OA imaging [14]. A miniaturized OA system combining a single red LD and an US array was used to image skin melanomas [15]. However, the US array adds cost and complexity to the system by necessitating many amplifiers and analog-to-digital-converters to record the OA signals. LD have also been used in OA microscopy with galvanometric [16] or stage scanning [17] to perform OA imaging. However, imaging increases the cost and the complexity of the OA systems for simple applications, such as measuring local vascular oxygenation. Single-point OA sensors employing a Nd:YAG laser equipped with an optical parametric oscillator (OPO) [18] have been introduced for measuring of blood oxygenation, but these light sources are expensive and bulky. OA spectroscopic sensors with low-cost LD have been developed to detect trace gases in the atmosphere [19] or for breath test analysis in human patients [20], but these cannot be applied to local vascular oxygenation sensing. To the best of our knowledge, there is no single-point OA spectroscopic sensor for the measurement of local vascular oxygenation that utilizes low-cost LD and is suited for point-of-care or bedside applications.

In this work, we introduce such a single-point spectroscopic optoacoustic sensor (SPOAS) for the measurement of local vascular oxygen saturation. We assumed that a single-point sensor (in comparison to imaging systems) could provide enough data to estimate the local vascular oxygenation accurately, thus reducing the device cost and size. SPOAS utilizes two low-cost miniaturized LD [21] operating at different wavelengths to estimate local vascular oxygenation non-invasively and in real time. We demonstrate the ability of the system to measure oxygen saturation values in blood and microvasculature in tissues by performing experiments on blood-phantoms and mice *in vivo*. We benchmark our prototype against standard invasive blood analysis devices, the BGA and OxyLite Pro. SPOAS is
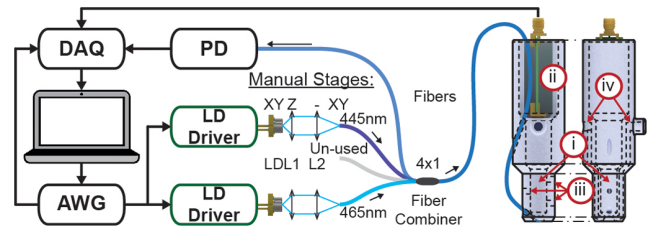

Fig. 1. Implementation of the multispectral hand-held optoacoustic device for the assessment of local tissue oxygenation. LD, laser diode; DAQ, data acquisition card; AWG, arbitrary waveform generator.

the first step toward a low-cost and miniaturized OA oximeter, which could be used alongside the standard pulse oximeter in the clinics to provide complementary measurements.

A personal computer and a custom-made program written in MATLAB (MATLAB 2018b, Mathworks, USA) controls the system. A two-channel arbitrary waveform generator (33522B, Keysight, USA) controls the LD driver, which is an upgraded version of a previously presented system [21]. The LD emit at 445 nm (LDM-448-3500, LaserTack, Germany) and 465 nm (LDM-465-3500, LaserTack, Germany), and they are installed in a XY-manual translation stage (CXY1, Thorlabs, USA). The collimating lens (C340TMD-A, Thorlabs, USA) was installed in a Z-manual translation stage (SM1Z, Thorlabs, USA). The focusing lens (C560TME-A, Thorlabs, USA) was kept stable, and the fiber was maintained in a second XY-manual stage. In this way, the output of the LD was efficiently (>90% coupling efficiency) coupled in a multimode fiber.

A custom-made 4×1 fiber power combiner was employed, with the input fibers being 200 μm and 0.22 NA (H26385704, LasFiberio, China). The LD were coupled into two of the four fibers of the combiner. The output of the fiber combiner consisted of a 400 μm, 0.22 NA fiber, which was used for the light delivery of both wavelengths to the sample. The third input fiber was used as an output to a fast photodiode (DET10A2, Thorlabs, USA), utilizing the small amount of back-scattered light (occurring at any input fiber) to monitor and correct for the pulse-per-pulse energy variation and small time jitters of the LD. The fourth channel was left free for potential upgrades.

The spherically focused ultrasound transducer (UST, I in Fig. 1, HFM29, Sonaxis, France) has a central frequency of 30 MHz, a 110% bandwidth, and an f-number of 1.07. The lateral resolution has been calculated at 110 μm, and the axial resolution 33 μm [21]. Taking into account the UST's spatial resolution and detection angle, we can estimate the interrogation volume to be ∼0.32 mm³ for a maximum penetration depth of ∼1 mm into tissue (the penetration depth is limited by the employed blue wavelength due to increased scattering and absorption). Currently, to the best of our knowledge, there are no commercially available LD in the green region that could offer a better signal-to-noise ratio (SNR) and penetration depth.

The UST and the output fiber were combined in a custom three-dimensional printed holder. The holder contained the custom-made voltage amplifier circuit (II), which includes two monolithic amplifiers (ERA − 8SM+, Minicircuits, USA), retaining screws to secure the position of the UST (III) and water delivery tubes (IV) for easy water coupling of the UST.

The OA signal after amplification, as well as the photodiode signal, was recorded by a high-speed digitizer (CSE1222,
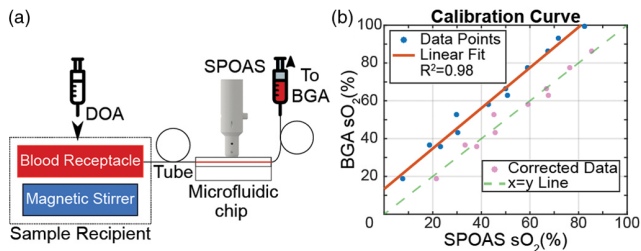
Fig. 2. System characterization and calibration. (a) Experimental scheme for oxygen saturation measurement in blood phantoms. DOA, deoxygenation agent; BGA, blood gas analyzer. (b) Probe calibration curve showing strong linear correlation between the values measured by the BGA and spectroscopic optoacoustic sensor and the same data, corrected to an $x = y$ line fit.

Fig. 3. Tissue blood oxygenation assessment of a mouse *in vivo*. (a) Location of measurement points on the mouse; (b)–(d) oxygen saturation obtained at points 1, 2, and 3 during an oxygen stress test.

GaGe, DynamicSignals LLC, USA) synchronized with the AWG. For all the OA measurements, we used a repetition rate of 250 kHz and 700 averages per wavelength, which resulted in ~15 measurements per second, including signal processing.

The size of the optical spot on the sample was measured with a CCD camera (daA1920-30um; Basler AG, Germany), and it was circular with a diameter of ~1 mm. The energy of the LD on the sample were determined to be 120 and 140 nJ for the 445 and 465 nm LD, respectively, using a thermal power meter (PM160T, Thorlabs, USA). Using the above-mentioned repetition rate and averages, the total exposure of the skin was calculated to be 8.3 μJ/cm^2 and 2.07 W/cm^2, less than the MPE limits of 20 mJ/cm^2 and 18 W/cm^2 imposed by the American National Standards Institute [22].

Figure 2 outlines the characterization of the SPOAS system, which was performed by measuring the oxygen saturation in blood phantoms. Figure 2(a) shows the experimental setup for the characterization. A volume of 50 ml of pure heparinized pig blood (Fiebig-Naehrstofftechnik, Germany) was placed inside a receptacle over a magnetic stirrer. The oxygen concentration of the blood phantoms was modified by mixing the blood with increasing amounts of a deoxygenation agent (DOA), which consisted of a concentrated solution of phosphate buffered saline (PBS) and sodium dithionite (Merck KGaG, Germany). The blood samples were directly drawn into a microfluidic chip (01-0173-0156-02, Microfluidics ChipShop, Germany), on which SPOAS was placed to monitor the oxygen concentration. Finally, the drawn blood samples were measured with a blood gas analyzer (BGA, Combiline, Medizintechnik Hadler & Braun GmbH, Germany).

The power of the optoacoustic signals has a linear dependency on the content volume of deoxyhemoglobin and oxyhemoglobin in the phantoms [10]. Figure 2(b) shows the oxygen saturation percentage for each blood phantom, as measured by the SPOAS probe and the BGA. The measurements from SPOAS have a strong linear correlation ($R^2 = 0.98$) with those from the BGA, which is the gold standard of blood analysis in the clinics. The linear fit gives a slope of 1.07 and offset of 13%, very close to the expected values of 1 and 0. The combination of the offset ($+13\%$) and the slightly higher slope (1.07) results in a SPOAS value of 80% for a 100% oxygen saturation according to the BGA. The same data were corrected to fit the $x = y$ line as shown in Fig. 2(b) (pink dots, green dashed line). We later use the linear fit (both the slope of 1.07 and the y-intercept of 13%) to correct the SPOAS data in the *in vivo* experiments.
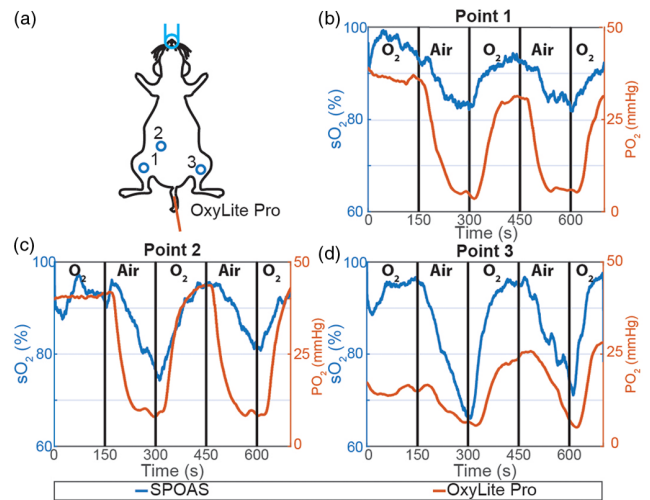
We then validated the ability of SPOAS to assess local vascular oxygenation in living mice (Fig. 3). All procedures with animals were approved by the District Government of Upper Bavaria. Figure 3(a) shows the sites on the mouse where measurements were recorded. As a control, an OxyLite Pro monitoring probe (Oxylite Pro—Oxford Optronix, UK) was positioned with a 22 G catheter in the tail vein to give real-time measurements of oxygen partial pressure (pO$_2$) in the blood. A BGA could not be used in this case, since it is calibrated for human red blood cells, which are larger than mouse red blood cells. The nude mouse (Athymic Fox-N1) was positioned on its back and was breathing a mix of isoflurane (for anesthesia) and two different concentrations of air: 0.9 lpm of 100% O$_2$ (O$_2$) and 0.9 l pm of 20% O$_2$ (Air). To monitor changes in the blood and local vascular oxygenation levels, we applied an oxygen stress test, wherein we alternated between pure O$_2$ and Air every 150 s for five cycles. The experiment was repeated three times at different parts of the body of the mouse, one in the lower part of each thigh and one in the belly, as shown in Fig. 3(a) as points 1, 3, and 2, respectively. All OA measurements were performed above the mouse skin and were non-invasive.

Figures 3(b)–3(d) show the results of the three stress tests at measurement points 1, 2, and 3. SPOAS provides values of local vascular oxygen saturation (sO$_2$), while (OxyLite Pro) provides values of oxygen partial pressure (pO$_2$) in the tail vein. Although there is a strong relationship between sO$_2$ and pO$_2$, temperature, pH, and the partial pressure of carbon dioxide (pCO$_2$) are required to convert between the two values. We present here only the pO$_2$ for the reference system, as the device only provided temperature measurements. Despite this, it can be seen in Figs. 3(b)–3(d) that SPOAS detects changes in the local vascular oxygenation (blue lines) in agreement with the reference instrument (orange lines). We also observe excellent agreement with the oxygen challenge. Specifically, we detected decreasing oxygenation during the Air period, which then recovers during the O$_2$ period. Moreover, the local vascular oxygen saturation as measured by SPOAS was around 95% during the O$_2$ period for all three measurement points. During the Air period, the local vascular oxygen saturation dropped to lower values—more than

85%, 75%, and 65% for Points 1, 2, and 3, respectively. These values are reasonable, as SPOAS measurements include both arterial and venous vessels, and since under normal conditions (Air), the typical oxygen saturation of arteries is over 95% and of veins between 65% and 75% [23]. The varying oxygen saturation values may then indicate that the concentration of arterioles and venules varied between the three points of measurement. From these results, we can infer that SPOAS is well calibrated and can provide absolute values of local vascular oxygenation for the first time from an OA system.

In this Letter, we presented a simple, non-invasive, spectroscopic optoacoustic sensor that can measure local vascular oxygenation, and benchmarked its performance against commercial blood analysis devices. Our system employs two small and inexpensive LD, which provide single-point, dual-wavelength, OA sensing to measure accurately local vascular oxygenation, while being non-invasive, handheld, and easy to use.

OA imaging systems with either galvanometric or stage scanning or with US arrays are commonly used to visualize the distribution of oxygenation of blood vessels in the tissue. However, here we showed that single point sensing can also provide sufficient information about the oxygen content of tissue microvasculature, without the need to generate images. SPOAS provides a mean oxygen saturation of the arterial and venous vessels located in the detection area with high accuracy. In this way, SPOAS can provide valuable information about the local vascular oxygen saturation and does not require scanning or an US array that would complicate the system and increase its cost.

SPOAS was calibrated using blood phantoms with controlled oxygenation and a BGA as the reference system, and it showed excellent linear correlation with the reference data [$R^2 = 0.98$, Fig. 1(b)]. SPOAS can accurately provide absolute values (rather that relative changes) of blood oxygen saturation, which has challenged many OA systems [24]. SPOAS was also validated *in vivo* in mice, with measurements at multiple locations showing excellent correlation with simultaneous measurements from an external reference device (Fig. 2). The accuracy of SPOAS can be further improved by correcting for spectral coloring [24].

SPOAS employs LD that require averaging over multiple pulses to increase the SNR; however, the high repetition rate of the lasers allows SPOAS to provide real-time data with an acquisition rate of ~15 Hz, fast enough to detect oxygenation changes, which usually happen in the range of tens of seconds.

To the best of our knowledge, SPOAS is the first example of a dedicated OA oximeter. The device can be miniaturized and is low cost, due to its use of inexpensive LD as excitation sources. However, only blue LD are currently available on the market; this limits the penetration depth in skin to less than ~1 mm. This limitation could be overcome by the entrance of high-power green LD in the market [25]. SPOAS could also be improved by the use of low-cost ultrasound detection devices such as a simple microphone [26]. Miniaturization of the necessary electronics for excitation, detection, and processing can further reduce the size and cost of the device. Clinical translation of the device will necessitate testing and calibration in humans, taking into account absorbers in human tissue, such as methemoglobin, myoglobin, and carboxyhemoglobin [27], as was done during the development of the pulse oximeter.

The optoacoustic sensor presented here, referred to as SPOAS, addresses the need to measure local vascular oxygenation using a low-cost and miniaturized device. Such a device, for which there is currently no alternative, could provide physicians with extremely valuable information alongside the pulse oximeter during surgery, emergency rescue, and other critical situations, thus improving treatment decisions.

Disclosures. Vasilis Ntziachristos is an equity owner and consultant for iThera Medical GmbH.

REFERENCES

1. V. De Santis and M. Singer, Br. J. Anaesth. **115**, 357 (2015).
2. A. Carreau, B. El Hafny-Rahbi, A. Matejuk, C. Grillon, and C. Kieda, J. Cell. Mol. Med. **15**, 1239 (2011).
3. G. L. Semenza, Annu. Rev. Pathol. Mech. Dis. **9**, 47 (2014).
4. S. J. Shepherd and R. M. Pearse, Anesthesiology **111**, 649 (2009).
5. T. W. L. Scheeren, P. Schober, and L. A. Schwarte, J. Clin. Monit. Comput. **26**, 279 (2012).
6. M. Ferrari, L. Mottola, and V. Quaresima, Can. J. Appl. Physiol. **29**, 463 (2004).
7. M. G. Lopez, P. Pandharipande, J. Morse, M. S. Shotwell, G. L. Milne, M. Pretorius, A. D. Shaw, L. J. Roberts, and F. T. Billings, Free Radic. Biol. Med. **103**, 192 (2017).
8. H. Lee, H. Ko, and J. Lee, ICT Express **2**, 195 (2016).
9. V. Ntziachristos and D. Razansky, Chem. Rev. **110**, 2783 (2010).
10. F. Cao, Z. Qiu, H. Li, and P. Lai, Appl. Sci. **7**, 1262 (2017).
11. P. Mohajerani, S. Tzoumas, A. Rosenthal, and V. Ntziachristos, IEEE Signal Process. Mag. **32**(1), 88 (2015).
12. M. Schwarz, A. Buehler, J. Aguirre, and V. Ntziachristos, J. Biophoton. **9**, 55 (2016).
13. M. Erfanzadeh and Q. Zhu, Photoacoustics **14**, 1 (2019).
14. Y. Zhu, G. Xu, J. Yuan, J. Jo, G. Gandikota, H. Demirci, T. Agano, N. Sato, Y. Shigeta, and X. Wang, Sci. Rep. **8**, 1 (2018).
15. S. Liu, K. Tang, H. Jin, R. Zhang, T. T. H. Kim, and Y. Zheng, Biomedical Circuits and Systems Conference (BioCAS) (2019).
16. M. Erfanzadeh, P. D. Kumavor, and Q. Zhu, Photoacoustics **9**, 1 (2018).
17. L. Zeng, Z. Piao, S. Huang, W. Jia, and Z. Chen, Opt. Express **23**, 31026 (2015).
18. A. Ray, J. R. Rajian, Y.-E. K. Lee, X. Wang, and R. Kopelman, J. Biomed. Opt. **17**, 057004 (2012).
19. P. Breitegger, B. Schweighofer, H. Wegleiter, M. Knoll, B. Lang, and A. Bergmann, Photoacoustics **18**, 100169 (2020).
20. M. Wolff, H. G. Groninga, and H. Harde, Smart Med. Biomed. Sens. Technol. **5261**, 50 (2004).
21. A. Stylogiannis, L. Prade, A. Buehler, J. Aguirre, G. Sergiadis, and V. Ntziachristos, Photoacoustics **9**, 31 (2018).
22. F. C. Delori, R. H. Webb, and D. H. Sliney, J. Opt. Soc. Am. A **24**, 1250 (2007).
23. E. P. Rivers, D. S. Ander, and D. Powell, Curr. Opin. Crit. Care **7**, 204 (2001).
24. Y. Li, Y. Tang, and J. Yao, Photoacoustics **10**, 65 (2018).
25. V. Perekatova, P. Subochev, M. Kleshnin, and I. Turchin, Biomed. Opt. Express **7**, 3979 (2016).
26. J. Y. Sim, C. G. Ahn, E. J. Jeong, and B. K. Kim, Sci. Rep. **8**, 1 (2018).
27. E. D. Chan, M. M. Chan, and M. M. Chan, Respir. Med. **107**, 789 (2013).